Molecular Immunology 111 (2019) 209–219

Contents lists available at ScienceDirect

Molecular Immunology

journal homepage: www.elsevier.com/locate/molimm

The mouse intron-nested gene, *Israa*, is expressed in the lymphoid organs and involved in T-cell activation and signaling

Noureddine Ben Khalaf[a], Wedad Al-Mashoor[a], Azhar Saeed[b], Dalal Al-Mehatab[a], Safa Taha[c], Moiz Bakhiet[c], M. Dahmani Fathallah[a,*]

[a] Department of Life Sciences, Health Biotechnology Program, College of Graduates Studies, Arabian Gulf University, Manama, Bahrain
[b] University of Michigan Medical School, MI, USA
[c] Department of Molecular Medicine, Princess Al-Jawhara Center for Genetics and Inherited Diseases, College of Medicine and Medical Sciences, Arabian Gulf University, Bahrain

ARTICLE INFO

Keywords:
T-cell activation
Nested gene
Gene expression
Elf1
Fyn
Yeast two-hybrid

ABSTRACT

We have previously reported *Israa*, *immune-system-released activating agent*, as a novel gene nested in intron 8 of the mouse *Zmiz1* gene. We have also shown that *Israa* encodes for a novel FYN-binding protein and might be involved in the regulation of T-cell activation. In this report, we demonstrate that *Israa* gene product regulates the expression of a pool of genes involved in T-cell activation and signaling. Real time PCR and GFP knock-in expression analysis showed that *Israa* is transcribed and expressed in the spleen mainly by $CD3^+CD8^+$ cells as well as in the thymus by $CD3^+$ (DP and DN), $CD4^+$SP and $CD8^+$SP cells at different developmental stages. We also showed that *Israa* is downregulated in T-cells following activation of T-cell receptor. Using yeast two-hybrid analysis, we identified ELF1, a transcription factor involved in T-cell regulation, as an ISRAA-binding partner. Transcriptomic analysis of an EL4 cell line overexpressing ISRAA revealed differential expression of several genes involved in T-cell signaling, activation and development. Among these genes, *Prkcb, Mib2, Fos, Ndfip2, Cxxc5, B2m, Gata3* and *Cd247* were upregulated whereas *Itk*, *Socs3*, *Tigit, Ifng, Il2ra* and *FoxJ1* were down-regulated. Our findings support the existence in mouse of a novel FYN-related T-cell regulation pathway involving the product of an intron-nested gene.

1. Introduction

Israa (GenBank: EU552928) is a novel mouse gene nested within intron 8 of the *Zmiz1* gene on chromosome 14. *Israa* was found to be over-expressed in splenocytes following *T. brucei* parasite inoculation to mice (Bakhiet and Taha, 2008). We also demonstrated this gene encodes for ISRAA; a novel FYN-binding protein and is likely to be involved in the regulation of T-cell activation through the phosphorylation of Src kinases Y416 activation residue (Ben Khalaf et al., 2016). Therefore, unravelling the molecular mechanisms by which the *Israa* gene product gets involved in the regulation of T-cell activation is likely to unveil novel immune response regulation and control pathway.

Israa belongs to this group of intron embedded or nested genes whose entire coding sequence lies within the chromosomal region bounded by the start and stop codons of a larger external gene. The presence of these unconventional genes was considered a neutral evolutionary process where large introns constituted an ideal niche for gene insertion (Hube and Francastel, 2015; Kumar, 2009). Since then, several reports have progressively shown that intron-nested genes have major biological functions other than self-regulation (Baggio et al., 2013; Cawthon et al., 1990; Salmeron et al., 1996). In human, Yu et al. (2005) identified 158 predicted protein-coding genes nested in introns within human genes. A human homologue of mouse *evi2a*, a gene involved in retro-virus induced murine myeloma, was shown to be nested in the Neurofibromatosis type 1 gene (*nf1*) and expressed in several tissues (Cawthon et al., 1990). Two other genes, *evi2b* and *ompg* are nested in the same intron and encode for EVI2B and an Oligodendrocyte-Myelin Glycoprotein (Viskochil et al., 1991). In *Drososphila melanogaster*, nested intronic genes represent approximately 6% of the organism's total number of genes, and 85% of these nested genes are predicted to encode proteins (Hube and Francastel, 2015). One of them, *2mit* was shown to be expressed in the nervous system and involved in behavioral plasticity (Baggio et al., 2013; Lee and Chang, 2013).

However, to our best knowledge, none of the known human or mouse intron-nested genes has so far been directly linked to the T-cell activation pathways or the immune response at large. T-cell activation

* Corresponding author.
E-mail address: d.fathallah@agu.edu.bh (M.D. Fathallah).

https://doi.org/10.1016/j.molimm.2019.04.006
Received 23 September 2018; Received in revised form 25 March 2019; Accepted 13 April 2019
Available online 13 May 2019

and differentiation is a turnkey in the process of immune regulation. T-lymphocytes play a central role in the immune response, both as direct effector cells and as regulatory cells that modulate the functions of numerous other cell types involved in organism's defense mechanisms. Undeniably, T-cells regulation and signaling are extremely complex process and involves an intricate network of essential and accessory molecules. T-cell activation manifests through measurable proliferation, differentiation, apoptosis, or cytokine release (Smith-Garvin et al., 2009). Upon T-cell receptor (TCR) interaction with the peptide-MHC complex, the associated CD3 chains undergo conformational changes leading to their phosphorylation via their c-terminal immune receptor tyrosine-based activation motifs (ITAMs) by the leukocyte-specific Src tyrosine kinases LCK and FYN (Laird and Hayes, 2010). Other signaling proteins like ZAP70 (Lin and Weiss, 2001) are then recruited, activated and phosphorylates adapter proteins LAT and SLP-76 resulting in activation of MAP-kinase and NFκB pathways (Samelson, 2002).

In this work, we carried out the profiling of *Israa* and its host gene, *Zmiz1*, expression in lymphoid organs and activated T-cells by generating an *Israa*-eGFP (enhanced Green Fluorescent Protein) knock-in mice strain and real-time PCR experiments. We also investigated the functional role of ISRAA in T-cell signaling following its phosphorylation by FYN using Yeast-two Hybrid screening and we identified ELF1, a transcription factor involved in T-cell signaling, as an ISRAA binding partner. In addition, transcriptomic analysis of a mouse lymphoblast T-cell line overexpressing the ISRAA protein revealed differential expression of a pool of genes involved in T-cell signaling and development. The evidences presented in this report, support the conclusion that *Israa* is the first described mouse intron-nested gene to encode for a signaling protein involved in T-cell activation and may reveal a novel pathway of immune response regulation.

2. Material and methods

2.1. Plasmids and primers

The DNA sequence encoding ISRAA protein was synthesized by GeneCust (GeneCust, Dudelange, Luxemburg) and sub-cloned into the pET-28a + system (Novagen, Madison, WI, USA) and p-SELECT-zeo (Thermo Fisher Scientific, Waltham, MA, USA) for N-terminal 6-His-tagged recombinant protein expression. pFloxin-IRES-eGFP was a gift from Jeremy Reiter (Addgene plasmid # 24557). Primers and probes used for genotyping, Southern blotting and real-time PCR are listed in Tables 1 and 2 .

2.2. Generation of israa-eGFP knock-in mice

Procedures and protocols used in the experiments involving animals were reviewed and approved by the Arabian Gulf University Ethic committee. The cloning and the initial generation of mice were conducted in collaboration with Genoway, Inc. (Lyon, France). The targeting strategy involved the insertion of an IRES-eGFP cassette downstream of the *Israa* coding sequence (CDS) along with insertion of *loxP* sites flanking the entire gene (exon 1 and exon 2) (Fig. 1A). The targeting construct was generated by sequential cloning of three homology arms harbouring the *israa* locus into a pFloxin-IRES-eGFP recipient plasmid (Addgene 24557). The three homology arms amplified from 129/Sv genomic DNA are as follows: 1- a 7082 bp fragment containing the *Israa* exon 1 non-coding sequence, exon 2 and its downstream sequence as a long homology arm (BKN1-LA); 2- a 1469 bp fragment containing the exon 1 CDS and upstream intronic sequence as a middle homology arm (BKN1-MA); and 3-a 2771 bp sized fragment containing the exon 1 upstream sequence as a short homology arm (BKN1-SA) (Fig. 1B). All isolated fragments were fully sequenced, and the sequences were compared between 129/Sv and C57BL/6 databases (Benson et al., 2005) to validate the absence of mutations and to identify any polymorphisms. No polymorphisms were reported in the exon coding region. The final targeting vector (BKN1-HR) and strategy have been depicted respectively in Fig. 1C and D.

The FseI linearized 21 kb-long BKN1-HR targeting construct (40 μg) was electroporated into 129/Sv ES cells (260 V, 500 μF). Following negative selection with G418, genomic DNA from surviving ES cell

Table 2
List of primers used for real-time PCR.

Primer	Sequence 5' to 3'
IL2RAF	CTCCCATGACAAATCGAGAAAGC
IL2RAR	ACTCTGTCCTTCCACGAAATGAT
FYBF	TCAACACGGGGAGTAACCC
FYBR	CGAGCTTTGTCCTGCAACT
ITKF	GGAAGAAGCGCACGTTGAAG
ITKR	ATGCACGACCTGAAAAGGGTA
IFNGF	ATGAACGCTACACACTGCATC
IFNGR	CCATCCTTTTGCCAGTTCCTC
FOXJ1F	CCCTGACGACGTGGACTATG
FOXJ1R	GCCGACAGAGTGATCTTGGT
PRKCBF	GTGTCAAGTCTGCTGCTTTGT
PRKCBR	GTAGGACTGGAGTACGTGTGG
NDFIP2F	GCAGCCGTCAACTTCTAGCTT
NDFIP2R	TAGCAACACTGTACGGAGGTG
MIB2F	CCCCGACCGTACAGTTGTC
MIB2R	TTTGGGCGTTGTCATAGAGCA
CXXC5F	CAGGAGGAACAGACAAAAGTACC
CXXC5R	GGCTCTTGTTGAGGGGTTCAC
SLC44A2F	GGACGCAGTCTATGGGACG
SLC44A2R	CCCTGTTGTAAATGGGTCCTTT
GATA3F	CTCGGCCATTCGTACATGGAA
GATA3R	GGATACCTCTGCACCGTAGC
FZD7F	CGGGGCCTCAAGGAGAGAA
FZD7R	GTCCCCTAAACCGAGCCAG
B2MF	TTCTGGTGCTTGTCTCACTGA
B2MR	CAGTATGTTCGGCTTCCCATTC
GAPHF	AGGTCGGTGTGAACGGATTTG
GAPDHR	TGTAGACCATGTAGTTGAGGTCA
SOCS3F	ATGGTCACCCACAGCAAGTTT
SOCS3R	TCCAGTAGAATCCGCTCTCCT
CD247F	TTCAGAACTCACAAGGACCCT
CD247R	GCTACTCTGCTGGGTGCTTTC
FOSF	CGGGTTTCAACGCCGACTA
FOSR	TTGGCACTAGAGACGGACAGA
TIGITF	GAATGGAACCTGAGGAGTCTCT
TIGITR	AGCAATGAAGCTCTCTAGGCT
ISRAAF	TGACCATGCAGAAGGAGACA
ISRAAR	GGAAGCGTGGAGAAGAACAA
ZMIZ1F	CCTGGGCTACAGACTCTTGG
ZMIZ1R	ATGGAGCTCATGGAGCTGAG

Table 1
List of primers and probes used for genotyping and Southern blot.

	Primer	Primer sequence 5' to 3'
Flpe-excision	125378flp-BKN1	CAACTGTCTTAGTTGGGTTTTTCACTATAGGACC
Genotyping	125379flp-BKN1	CTACAATTTCCAGGTTATTGGAGATCCAGG
5'-SA-E-A probe	125370PRO-BKN1	GCCAGAGGCAGAGAATACAGTTTAGAGACG
	125371PRO-BKN1	CCTTTCCCGGAGCTTATTAATGAGGTTCTA
3'-LA-I-C	125403PRO-BKN1	GAGCCCACCTCATGTCAGCATAAGC
Probe	125404PRO-BKN1	CCATTTGCCAGGTATCCAGACCTCC

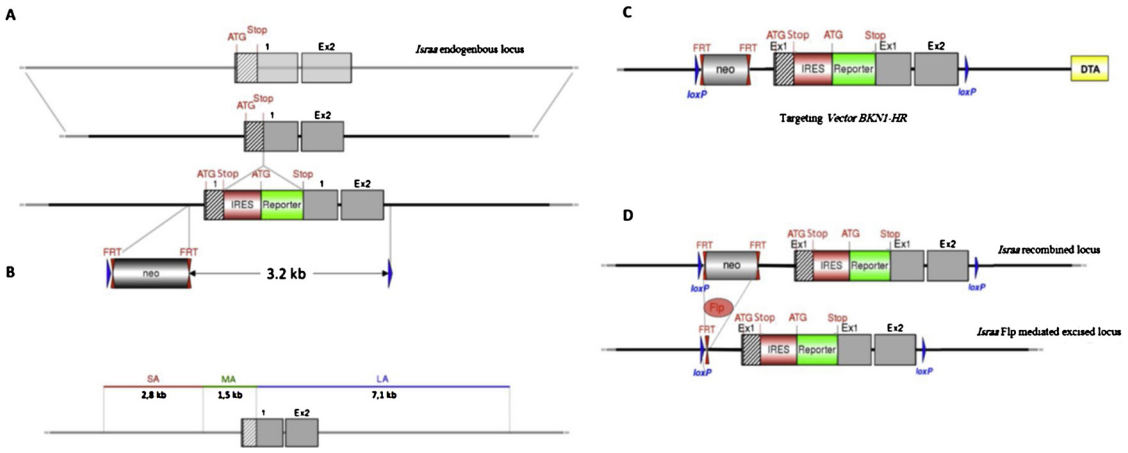

Fig. 1. *Israa* gene targeting strategy. Diagram is not depicted to scale. Hatched rectangles represent *Israa* coding sequences, grey rectangles indicate non-coding exon portions, red and green rectangles represent respectively IRES and reporter (eGFP, ref: addgene 24557) cassettes, solid lines represent chromosome sequences. *loxP* sites are represented by blue triangles and FRT sites by double red triangles. The initiation (ATG) and Stop (Stop) codons are indicated. The size of the flanked *Israa* sequence to be deleted is specified. (**A**) IRES-eGFP cassette is inserted downstream of stop codon in the *israa* CDS. FRT-flanked neomycin resistance gene is inserted upstream of the *Israa* locus. The entire targeting cassette is *loxP*-flanked (blue triangle). (**B**) Targeting vector design. SA, short arm; MA, middle arm and LA, long arm. (**C**) Targeting vector BKN1-HR. (**D**) Flpe-mediated excision of the neomycin resistance cassette. DTA, Diphteria Toxin A negative selection marker, FRT, flippase recognition target sites; FLPe, flippase; IRES, internal ribosome entry site, neo, neomycine resistance gene. (For interpretation of the references to colour in this figure legend, the reader is referred to the web version of this article).

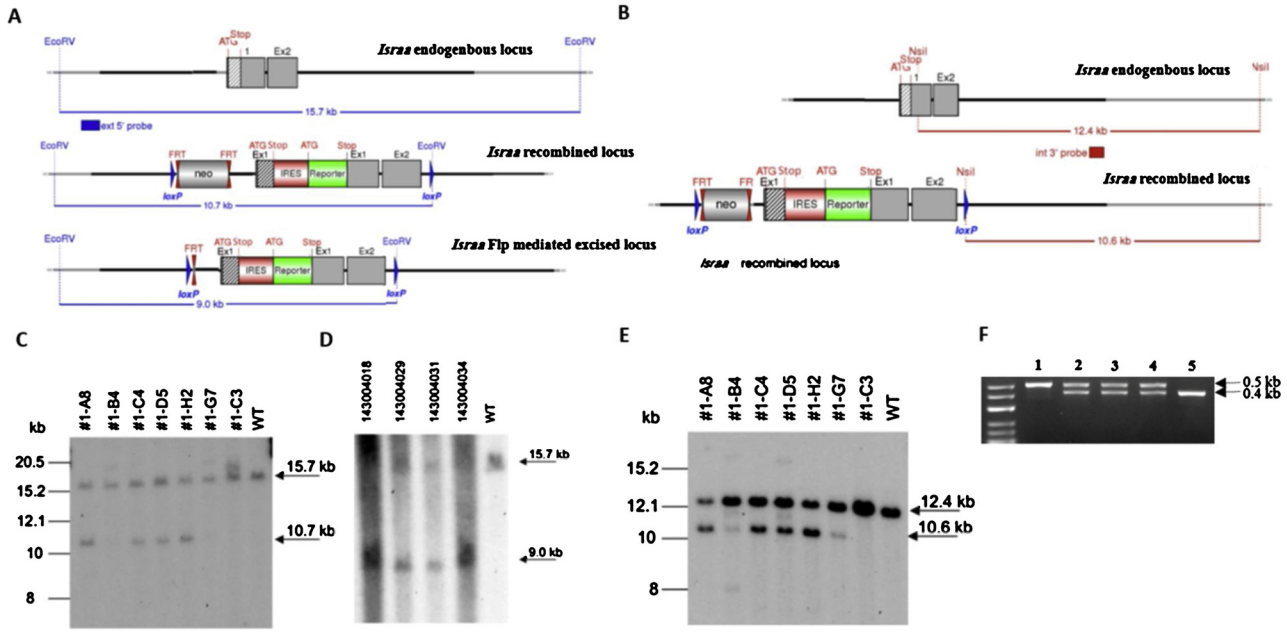

Fig. 2. Southern Blot strategy for recombination event detection and PCR strategy for genotyping. Diagram is not depicted to scale. Hatched rectangles represent *Israa* coding sequences, grey rectangles indicate non-coding exon portions, red and green rectangles represent respectively IRES and reporter (eGFP, ref: addgene 24,557) cassettes, solid lines represent chromosome sequences. *loxP* sites are represented by blue triangles and FRT sites by double red triangles. The initiation (ATG) and Stop (Stop) codons are indicated (**A**) Schematic representation of the wild-type, recombined and *Flp*-mediated excised *Israa* alleles with the relevant restriction sites for the Southern blot detection of the 5′-targeting event. (**B**) Schematic representation of the wild-type *Israa* allele and the recombined allele with the relevant restriction sites for the Southern blot analysis. The strategy for the Southern blot detection of the 3'-targeting event is indicated. (**C**) Southern blot analysis for 5′ homologous recombination in ES cells. The genomic DNA of the tested ES cell clones was compared with Sv129 wild-type DNA (WT). (**D**) Southern blot analysis of the heterozygous Neo-excised conditional reporter mice compared to C57BL/6 wild-type genomic DNA (WT). (**E**) Southern blot analysis for 3' homologous recombination in ES cells compared with Sv129 wild-type DNA (WT). (**F**) PCR identification of the Flp-mediated excision event within the recombined *Israa* locus. The optimised PCR screen was tested on wild-type (lane1), heterozygous (lanes 2–4) and homozygous *Israa*-eGFP mice (lane 5). (For interpretation of the references to colour in this figure legend, the reader is referred to the web version of this article).

colonies was used to screen for homologous recombination by Southern hybridization. Southern blot screening of 5′ recombination was based on an EcoRV digestion of the genomic DNA and hybridization using an external 5′ probe (SA-E-A probe) located upstream of the targeting vector homology sequence (Fig. 2A). Southern blot screening of 3' recombination was based on an NsiI digestion of the genomic DNA and hybridization using an internal 3' probe (LA-I-C probe) located within the targeting vector 3′ homology sequence (Fig. 2B). The initial 5′-recombination screening revealed 20 positive clones displaying an amplified product at the expected size of 3270 bp. Seven of the recombined clones identified by PCR were further verified by Southern blot analysis for 3' homologous recombination verification. The correctly targeted ES

cell clones were injected into C57BL/6J blastocysts and chimaeras were crossed with *β-actin–Flpe* transgenic mice [strain name: B6.Cg-Tg (ACTFLPe) 9205Dym/J; stock no.: 005703; The Jackson Laboratory] to excise the neomycin selection cassette and generate the *Israa-eGFP*$^{+/flox}$ allele. F1 heterozygous males were further validated by PCR and Southern blot and backcrossed for 8 generations with C57BL/6 J wild-type mice. Backcrossed heterozygous mice were intercrossed to generate homozygous *Israa-eGFP*$^{flox/flox}$ mice.

2.3. Genotyping

PCR for genotyping mice was performed on genomic DNA prepared from tail snips or ear clippings using the DNeasy Blood and Tissue kit® (QIAGEN, USA). Briefly, mouse biopsies were lysed and genomic DNA was isolated and used for genotyping reaction. For the detection of the Flpe-mediated recombination, the 125378flp-BKN1/125379flp-BKN1 primer set (Table 1) was used to amplify the Flpe-recombined (511 bp) and wild type (427 bp) alleles (Fig. 2F).

2.4. Analysis of GFP expression in Israa-eGFP knock-in mice

8-week-old *Israa-eGFP* knock-in mice (n = 5) and wild-type mice (n = 1) were fed a pre-imaging AIN-93 M diet for one week prior to experimentation to limit autofluorescence. Whole-body (anterior and posterior) imaging was performed on shaved, euthanized mice. The Lumina Ivis imaging system (Perkin Elmer, USA) was used to detect epi-fluorescence with medium and small binning using a 5-second acquisition time. The following wavelengths were used: excitation, 445–490 nm; emission, 515–575 nm and autofluorescence, 410–440 nm. Images were analysed using the Living Image 4.4 software (PerkinElmer). Upon completion of imaging, *Israa-eGFP* knock-in mice (n = 2) were euthanized and different organs were analysed *ex-vivo*. The results were expressed as the average radiant efficiency ([p/s/cm^2/sr] / [μW/cm^2]) fold increase in *Israa-eGFP* mice tissues compared with wild type. Freshly excised tissues were sectioned using a microtome. 5 μm sections were stained with DAPI and GFP expression was observed using the EVOS FL Cell Imaging System (Life Technologies). For immunofluorescence, Anti-CD3 antibody [EP4426] (Alexa Fluor® 647) (Abcam ab198937) was used, sections were stained with DAPI and mounted using Vectashield mounting medium (Vector Laboratories). Images were acquired on Zeiss Axio Observer Z1 Inverted Fluorescence Microscope.

2.5. Multiplex immunohistochemistry

Immunohistochemistry staining was performed on the Ventana Discovery Ultra Chromogenic AmpHQ automated immunostainer (Ventana Medical Systems, Tucson, AZ, USA) to investigate T-cell subpopulations expressing GFP in Thymus and spleen 5 μm sections from 3 weeks old female *Israa-eGFP* mice. The multiplex technology uses sequential application of unmodified primary antibodies with a specific heat deactivation steps in between that does not affect epitope in the tissue. In a sequential staining procedure, deactivation of the primary antibody and secondary antibody-HRP/AP bound to the first biomarker, prior to the application of subsequent biomarker(s), is critical to reducing cross-reactivity and facilitating downstream image analysis. The Cell Conditioning2 buffer (CC2, #950-123, Ventana, Tucson, AZ, USA) was used for deactivation of the bound primary antibody and secondary antibody-HRP, while maintaining the integrity of the tissue morphology and the subsequent epitopes. Deparaffinization and on-board antigen retrieval were performed for 64 min at 95∘C with the CC1 reagent (#950-500, Ventana). Slides were coloured using VENTANA reagents except as noted, according to the manufacturer's instructions. For the T-cells a 2-Plex protocol was used, two pre-diluted primary antibodies were sequentially applied in the following order using the indicated chromogenic detection: rabbit anti-GFP (1:200, Abcam ab6556) with ChromoMapDAB (#760-159) and rabbit Anti-CD3 antibody (1:200, Abcam ab5690) with Discovery Teal-HRP (#760-247). For the T-cell subpopulation study a 4-Plex protocol was used, four pre-diluted primary antibodies were sequentially applied in the following order using the indicated chromogenic detection: anti-FoxP3 (1:200, CST 98377S) with ChromoMapDAB (#760-159), rabbit anti-CD4 (1:200, Abcam ab183685) with Discovery Teal-HRP (#760-247), rabbit anti-CD8 (1:200, Abcam ab217344) with Discovery Purple (#760-229), and rabbit anti-GFP (1:200, Abcam ab6556) with Discovery Yellow AP (#760-239). Finally, the slides were counterstained with hematoxylin and bluing reagent according to the manufacturer recommendations. Images acquisition and quantitative analysis were performed using HALO™ Image Analysis Software (Perkin Elmer).

2.6. T-cell proliferation assay

Spleen was isolated from two 8 weeks old female C57BL/6J mice, and homogenized using 40 μm cell strainer (Corning, USA). Red blood cells (RBC) were lysate using RBC lysis buffer (Biovision Inc., CA, USA) and lymphocytes were washed twice in PBS1×. T-cells were isolated using Dynabeads™ FlowComp™ Mouse Pan T (CD90.2) Kit (Thermofischer Scientific, USA) according to the manufacturer recommendation. For the activation assay, Dynabeads® Mouse T-Activator CD3/CD28 kit (Thermofischer, USA) was used. Briefly, 8.10^4 purified T-cells were incubated with 2 μl of pre-washed magnetic beads and incubated at 37 °C, 5% CO_2 in a humidified incubator. Proliferation was assayed using CellTiter-Glo® Luminescent Cell Viability Assay (Promega, USA) after 48 and 72 h of incubation, according to the manufacturer instructions, luminescence was measured using GloMax® Discover Multimode Microplate Reader (Promega, USA). Experiments were run in triplicates and results were expressed as stimulation index using unstimulated cells as reference.

2.7. Analysis of Zmiz1 and Israa mRNA expression

Thymus tissues were isolated from 4-, 6- and 8- weeks old C57BL/6 female mice. Purified T-cells from spleen were activated as described above and harvested for RNA extraction. Total mRNA was extracted from homogenized tissues using the RNeasy RNA extraction kit (QIAGEN) and reverse transcribed using the ProtoScript® First Strand cDNA Synthesis Kit (NEB, UK) according to the manufacturer's instructions. Primer sets for real-time PCR (Table 2) were designed to amplify the region encompassing the junction between exons 8 and 9 junction of *Zmiz1* and *Israa* open reading frame (ORF) using the PowerUp Sybr Green Master Mix (Applied Biosystems). Experiments were run in triplicates and results were expressed as the fold change ($2^{-\Delta\Delta ct}$ method) using GAPDH as a housekeeping gene and week-4 thymus *Zmiz1* gene expression as reference.

2.8. Yeast two-hybrid screen

Y2H screening was performed in collaboration with Hybrigenics Services (Paris, France). The mouse *Israa* coding sequence was amplified by PCR and cloned into pB27 as a C-terminal fusion to LexA (N-LexA-Israa-C). The construct was used as a bait to screen a randomly primed mouse spleen cDNA library constructed in the pB27 and pP6 plasmids and derived from the parental pBTM116 (Vojtek and Hollenberg, 1995) and pGADGH (Vojtek and Hollenberg, 1995) plasmids, respectively. One hundred million clones (10-fold the complexity of the library) were screened using a mating approach with the YHGX13 (Y187 ade2-101::loxP-kanMX-loxP, matα) and L40ΔGal4 (matα) yeast strains expressing Fyn kinase as previously described (Bartel et al., 1993). In the initial tests, the bait fusion was neither toxic nor significantly auto-activating. Two rounds of screening were performed and a total of 154 His + colonies were selected from a medium lacking tryptophan, leucine and histidine. The prey fragments from the

positive clones were amplified by PCR and sequenced at their 5′- and 3' junctions. The resulting sequences were used to identify the corresponding interacting proteins from the GenBank database (Benson et al., 2005). A confidence score (PBS, Predicted Biological Score) was attributed to each interaction as previously described (Fromont-Racine et al., 1997). GO Molecular function annotation was performed for the resulting sequences using the Blast2GO software (Gotz et al., 2008).

2.9. Cell culture and stable cell line generation

EL4 (*Mus musculus* lymphoma, ATCC ID: TIB 39) mouse T-cell lymphoma cells were maintained in Dulbecco's modified Eagle's medium (DMEM) (Sigma-Aldrich, St. Louis, MO, USA) supplemented with 10% horse serum (Gibco, Gaithersburg, MD, USA), 0.1 mg/ml streptomycin and 100 U/ml penicillin at 37 °C with 5% CO_2. Cells were grown to reach a density of 2.5×10^6 cells/ml. A total of 2×10^7 cells were mixed with 10 µg of either p-SELECT-zeo-ISRAA expressing N-terminal 6His-tagged ISRAA or p-SELECT-zeo-eGFP. The cell suspension (0.4 ml) was subjected to electroporation using a BTX Electro Cell Manipulator with the following parameters; 140 V, 720 Ohms, and 3175 µF, across a BTX cuvette with a 0.2 cm electrode gap. Pulse lengths varied between 25 and 28 ms. Electroporated cells were incubated at room temperature for 15 min, then transferred to complete medium and returned to the cell culture incubator. Zeocin was subsequently added for selection at concentrations ranging from 100 to 200 µg/ml. The electroporation efficiency was assessed by fluorescence microscopy with the p-SELECT-zeo-eGFP electroporated live cells. Ten days after transfection, 2×10^5 cells were harvested and assayed for recombinant ISRAA expression by Western blotting and total RNA extraction.

2.10. Co-immunoprecipitation and Western blot analysis

EL4 cells stably expressing ISRAA were cultivated in DMEM (Sigma-Aldrich, St. Louis, MO, USA) supplemented with 10% horse serum (Gibco, Gaithersburg, MD, USA), and 200 µg/ml Zeocin at 37 °C with 5% CO_2 for 48 h and lysed in NP-40 lysis buffer. Non-electroporated EL4 cells were used as negative control. Cell lysates were incubated with 10 µg of mouse anti-ISRAA monoclonal antibody developed by GenScript (GenScript, NJ, USA) overnight at 4 °C then with Pierce™ Protein A/G Magnetic Beads (Thermo Fisher Scientific, MA, USA) for 1 h at room temperature. Antibody-linked protein complexes were then eluted and resolved by SDS-PAGE, followed by Western blotting for ELF1, eEF1A1, TENC1 and PLAGL2 using specific antibodies (cat. # ab64937, ab96381, ab116325, and ab139509, Abcam, Cambridge, UK) at a final dilution of 1:1000. Anti-rabbit and anti-mouse IgG coupled to HRP (Cell Signaling Technology, Danvers, MA, USA) were used as secondary antibodies at a final dilution of 1:2000. Bands were detected using an enhanced chemiluminescence kit (GE Healthcare, Buckinghamshire, UK) and membranes were scanned with an image analyser (LAS-1000, Fuji Film, Tokyo, Japan).

2.11. Transcriptome library preparation and Illumina sequencing

For RNA-seq analysis, 5 µg of total RNA was isolated using an RNeasy Mini kit (QIAGEN) according to the manufacturer's recommendations. RNA purification, reverse transcription, library construction and sequencing were performed according to the manufacturer's instructions (Illumina, San Diego, CA). Two RNA-seq transcriptome libraries (ISRAA-expressing EL4 cells and non-electroporated control EL4 cells) were prepared using a modified Illumina TruSeq RNA Sample Preparation protocol. The first step involves the removal of ribosomal RNA (rRNA) using biotinylated, target-specific oligos combined with Ribo-Zero rRNA removal beads. The Ribo-Zero Gold kit (Illumina, San Diego, CA) depletes samples of both cytoplasmic and mitochondrial rRNA. Following purification, the mRNA is fragmented using divalent cations under elevated temperature. Taking these short fragments as templates, double-stranded cDNA was synthesized using a SuperScript double-stranded cDNA synthesis kit (Invitrogen, CA) with random hexamer primers (Illumina, USA). Then, the synthesized cDNA was subjected to end-repair, phosphorylation, 'A' base addition and ligation of the adapters according to Illumina's library construction protocol. Libraries were size- selected for 200–300 bp cDNA target fragments on 2% Low-Range Ultra Agarose followed by PCR amplification using Phusion DNA polymerase (New England Biolabs, Boston, MA). The two RNA-seq libraries were then sequenced on an Illumina Hiseq 2500 sequencer (Illumina, San Diego, CA), generating 20 million 2×100 bp paired-end reads (Cock et al., 2010; Erlich et al., 2008).

2.12. Sequencing data assembly and functional annotation

Image data output from the sequencer was transformed into raw reads by base calling and stored in FASTQ format. Based on the FastQ file quality report, the sequence reads were trimmed to include only high quality sequences for further analysis. Adapter trimming was performed using the Trimmomatic program (version - 0.36). Non-polyA-tailed RNAs, mitochondrial genome sequences, ribosomal RNAs and transfer RNAs were aligned using Bowtie2 (version - 2.2.4). The paired-end reads are aligned to the reference mouse genome release downloaded from the Ensembl database (ftp://ftp.ensembl.org/pub/release89/fasta/mus_musculus/dna/Mus_musculus.GRCm38.dna.toplevel.fa.gz). The GTF file was downloaded from ftp://ftp.ensembl.org/pub/release-89/regulation/mus_musculus/mus_musculus.GRCm38.Regulatory_Build.regulatory_features.20161111.gff.gz. Alignment was performed using the HISAT (fast spliced aligner) program (version HISAT_0.1.7). The aligned reads were used for estimating gene expression using featureCounts (version - 1.5.2). Differential expression analysis was performed using DESeq2. Differentially expressed genes were selected with fold change values between -0.55 and 1.8. DAVID annotation was performed for the differentially expressed genes. Biological processes, molecular functions and cellular components were described by the GO annotations using DAVID (https://david.ncifcrf.gov/). The KEGG database (http://www.genome.jp/kegg/) was used to predict possible functional classifications and metabolic pathways. RNA-seq data have been deposited in the ArrayExpress database at EMBL-EBI (www.ebi.ac.uk/arrayexpress) under accession number E-MTAB-6979.

2.13. Real time PCR validation of differentially expressed genes

Total mRNA was extracted from EL4 and EL4-Israa cell lines using the RNeasy RNA extraction kit (QIAGEN) and reverse transcribed using the ProtoScript® First Strand cDNA Synthesis Kit (NEB, UK) according to the manufacturer's instructions. Primers and probes for real-time PCR were designed to specifically amplify target genes using the PowerUp Sybr Green Master Mix (Applied Biosystems) (Table 3). Two experiments were run independently in triplicates and the results were expressed as the fold change ($2^{-\Delta\Delta ct}$) using GAPDH as a housekeeping

Table 3
List of genes identified by yeast two-hybrid screening using ISRAA as the bait against a mouse splenocyte library. PBS, Predicted Biological Score. SID, Selected Interacting Domain.

Gene	Gene ID (NCBI)	Global PBS	SID (Residues)	Pfams
Eef1a1	13627	A	301-368	PF00009, PF03143
Elf1	13709	B	425-495	Not annotated
Plagl2	54711	C	169-449	PF13465, PF13465, PF13465, PF13894
Tenc1	209039	C	1055-1338	PF00017, PF08416

gene.

3. Results

3.1. Generation of an Israa-eGFP knock-in mice

To monitor *Israa* gene expression, *Israa-eGFP* knock-in mice were created by the insertion of an *IRES-eGFP* cassette downstream of the stop codon in the CDS present in exon 1 of the *Israa* gene (Fig. 2A). The gene targeting construct was introduced into ES cells to obtain heterozygous *Israa-eGFP*$^{+/flox}$ ES clones by homologous recombination, which was verified by Southern blot and PCR (Fig. 2B, C and E). *Israa-eGFP*$^{+/flox}$ ES cells were injected into mouse blastocysts and homozygous *Israa-eGFP*$^{flox/flox}$ mice were obtained using standard procedures. Genotypes of *Israa-eGFP*$^{flox/flox}$ mice were validated by PCR screening (Fig. 2F).

3.2. GFP is expressed in mouse brain, testis, spleen and thymus

To analyse tissue-wide expression of ISRAA, *in vivo* imaging was performed on *Israa-eGFP*$^{flox/flox}$ mice. Increase in fluorescence corresponding to a fold change > 1 in average radiant efficiency was observed in the kidney, brain, testis, spleen and thymus of *Israa-eGFP* knock-in mice in comparison to wild-type mice (Fig. 3A), intestines signal was not considered due to food fluorescence.

3.3. ISRAA is expressed in T-cell subpopulations and downregulated in activated T-cells

Multiplex Immunofluorescence (IF) and Immunohistochemistry (IHC) studies were performed on *Israa-eGFP*$^{flox/flox}$ 3-week-old female mice. IF showed that GFP and CD3 colocalize (Fig. 3B) mainly in the white pulp area of the spleen (Fig. 3C) and the medulla area of the thymus (Fig. 3D). Immunohistochemistry study (Fig. 4) confirmed that almost the totality of CD3+ thymic cells express GFP (Fig. 4A, B and E), while half of GFP + splenic cells are CD3+ (Fig. 4C, D and E). Further investigation of differentiation markers of T-cells in the thymus (CD4, CD8 and Foxp3) (Fig. 5A and B) showed no colocalization of Foxp3 and GFP, while a proportion of SP CD4+ (40%) and CD8+ (75%) cells, express GFP (Fig. 5E). In the spleen (Fig. 5C and C), only 10% of SP CD4+ cells and 30% of SP CD8+ cells express GFP (Fig. 5E). Interestingly, a small proportion of DP cells (CD4+CD8+) (less than 1% of total cells) express GFP in both tissues. Meanwhile, in wild type mice, real time PCR confirmed the overexpression of *Israa* gene compared to *Zmiz1* during thymus maturation stages (4, 6 and 8 weeks), with up to 22 fold increase higher than Z*miz1* expression which was stable during these stages (Fig. 6A). CD3/CD28 stimulated cells showed a significant proliferation with a stimulation index of 3.5 and 15 at 48 and 72 h respectively, compared to unstimulated cells (Fig. 6B). Real time PCR showed that *Israa* is downregulated more than 2.5 times in CD3/CD28 activated T-cells after 48 h of stimulation, compared to unstimulated cells, whilst no significant change in *Zmiz1* was observed (Fig. 6C).

3.4. ISRAA binds to the transcription factor ELF1

To identify ISRAA-interacting proteins that may contribute to its functions, we used *Israa* cDNA-encoded protein as bait to screen a randomly primed mouse spleen cDNA library. We showed previously that FYN kinase phosphorylates ISRAA's Y_{102} which may be important for subsequent interaction of the protein. For this purpose, FYN kinase was co-expressed with the bait protein to ensure phosphorylation of the Y_{102} residue of ISRAA. A total of 28 proteins were identified. GO annotation analysis for molecular functions using the Blast2GO software identified 23 proteins with binding functions (GO:0005488), three of which had transcription factor activity and protein binding functions (GO:0000988) and seven of which had nucleic acid binding transcription factor activities (GO:0003700). Eight proteins had catalytic activities (GO:0003824) and two were associated with regulator functions (GO:0098772). Proteins with PBS scores ranging from A to C (Table 3) were selected for further validation.

To validate these 4 proteins as ISRAA-interacting partners, co-immunoprecipitation was carried out in cell lysates prepared from EL4 cells stably over-expressing recombinant ISRAA. Western blotting revealed ISRAA to be expressed in a monomeric form with a molecular weight of approximately 15 kDa, as expected (Fig. 7A). ISRAA expression was not detected in control cells (Fig. 7A). Cell lysates were subjected to immunoprecipitation with mouse anti-ISRAA monoclonal antibody, followed by Western blotting for ELF1, eEF1 A1, TENC1 and PLAGL2. Of these 4 potential interacting partners, only ELF1 co-immunoprecipitated with ISRAA at a detectable level (Fig. 7B). ELF1 was detected as a 67 kDa band, similar to the band detected in control lysates. We here confirmed the transcription factor ELF1 as a novel binding partner of ISRAA.

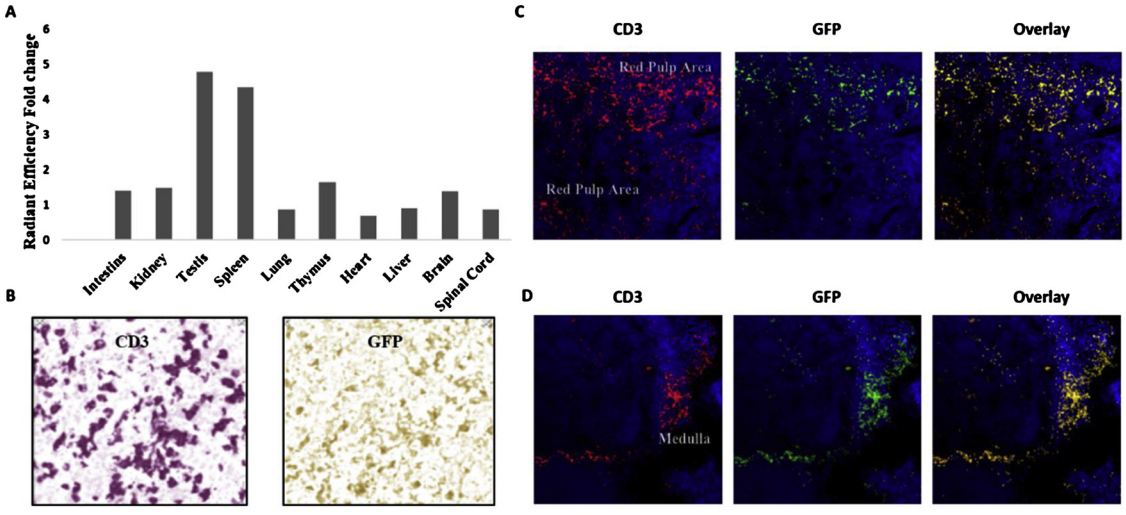

Fig. 3. Analysis of GFP expression in Israa-eGFP knock-in mice. (A) Signal quantification from in vivo imaging. Increased fluorescence in testes, brain, spleen and thymus of Israa-eGFP knock-in mice. (B) Immunofluorescence detection of CD3 (red), GFP (green) on thymus section (40X) (C) Immunofluorescence detection of CD3 (red), GFP (green) and overlay co-localization of CD3 and GFP (yellow) in spleen white pulp area and (D) thymus medulla regions, DAPI staining in blue. (For interpretation of the references to colour in this figure legend, the reader is referred to the web version of this article).

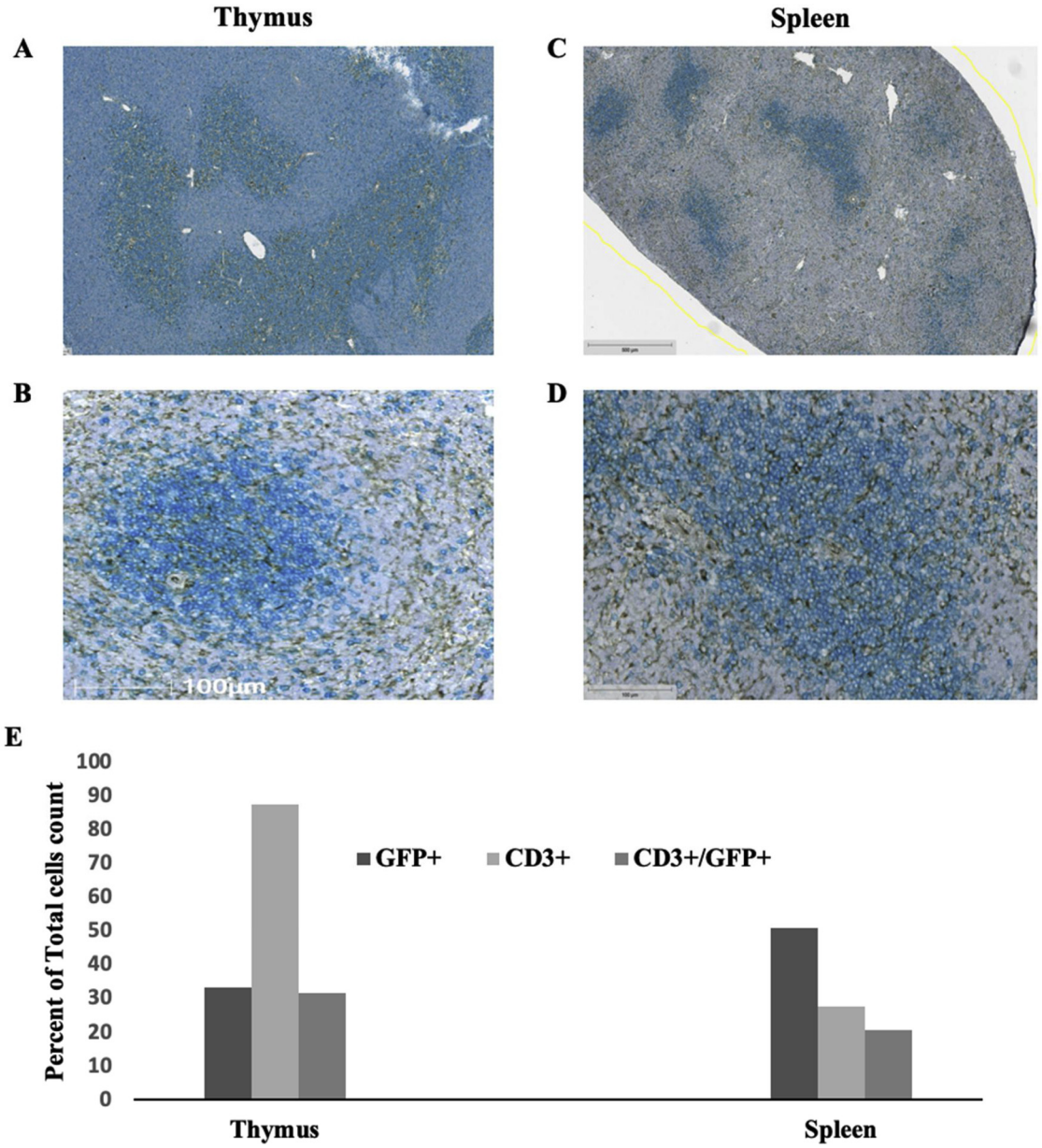

Fig. 4. Immunohistochemistry study of lymphoid tissues sections of (A, B) Thymus and (C, D) Spleen sections, for the detection of CD3 (Teal), GFP (Brown) and colocalization of both (dark blue). (E) Percentage of GFP+, CD3+ and GFP + CD3+ cells from total cell count in Thymus and Spleen sections. (For interpretation of the references to colour in this figure legend, the reader is referred to the web version of this article).

3.5. Transcriptomic analysis reveals potential roles for ISRAA in T-cell signaling and activation regulation

In order to further understand the role of *Israa* in cell signaling and gene expression regulation, two RNA-seq transcriptome libraries (ISRAA-expressing EL4 cells and mock-transfected control EL4 cells) were prepared and sequenced on an Illumina Hiseq 2500 sequencer (Illumina, San Diego, CA), generating 20 million 2 × 100 bp paired-end reads. FastQ file analysis showed a minimum average PHRED score of 38.4, a mean read length of 100 bp and a satisfactory base and GC content distribution for the samples. The GRCm38 mouse genome release was used to align the contamination-free reads, and differential gene expression analysis was performed using the Deseq2 software (Fig. 8A). Differentially expressed genes that showed fold change between chosen cut-off values of 0.55 and 1.8 (with $p \leq 0.05$) were selected for further analysis. A total of 276 genes were shown to be differentially regulated, with 140 up-regulated and 136 down-regulated genes. DAVID Gene Ontology analysis showed 18 genes (˜6.5%) displaying GO molecular functions related to transcription factor complex formation and transcription regulation (GO:0001077, GO:0000979, GO:0001046 and GO:0000976), 16 genes (˜6%) encoding for signal transduction proteins (GO:0004871) and 11 genes (˜4%) encoding for kinase binding proteins (GO:0019901). Using real time PCR we validated several genes involved in T-cell signaling, activation and differentiation to be differentially regulated (Fig. 8B). Among these genes, *Prkcb, Mib2, Fos, Ndfip2, Cxxc5, B2m, Gata3* and *Cd247* were upregulated whereas *Itk*, *Socs3*, *Tigit, Ifng*, *Il2ra* and *FoxJ1* were down-regulated. These findings suggest that *Israa* is involved in the expression regulation of genes related to several pathways in the immune cell activation and differentiation that will be further discussed in the following section.

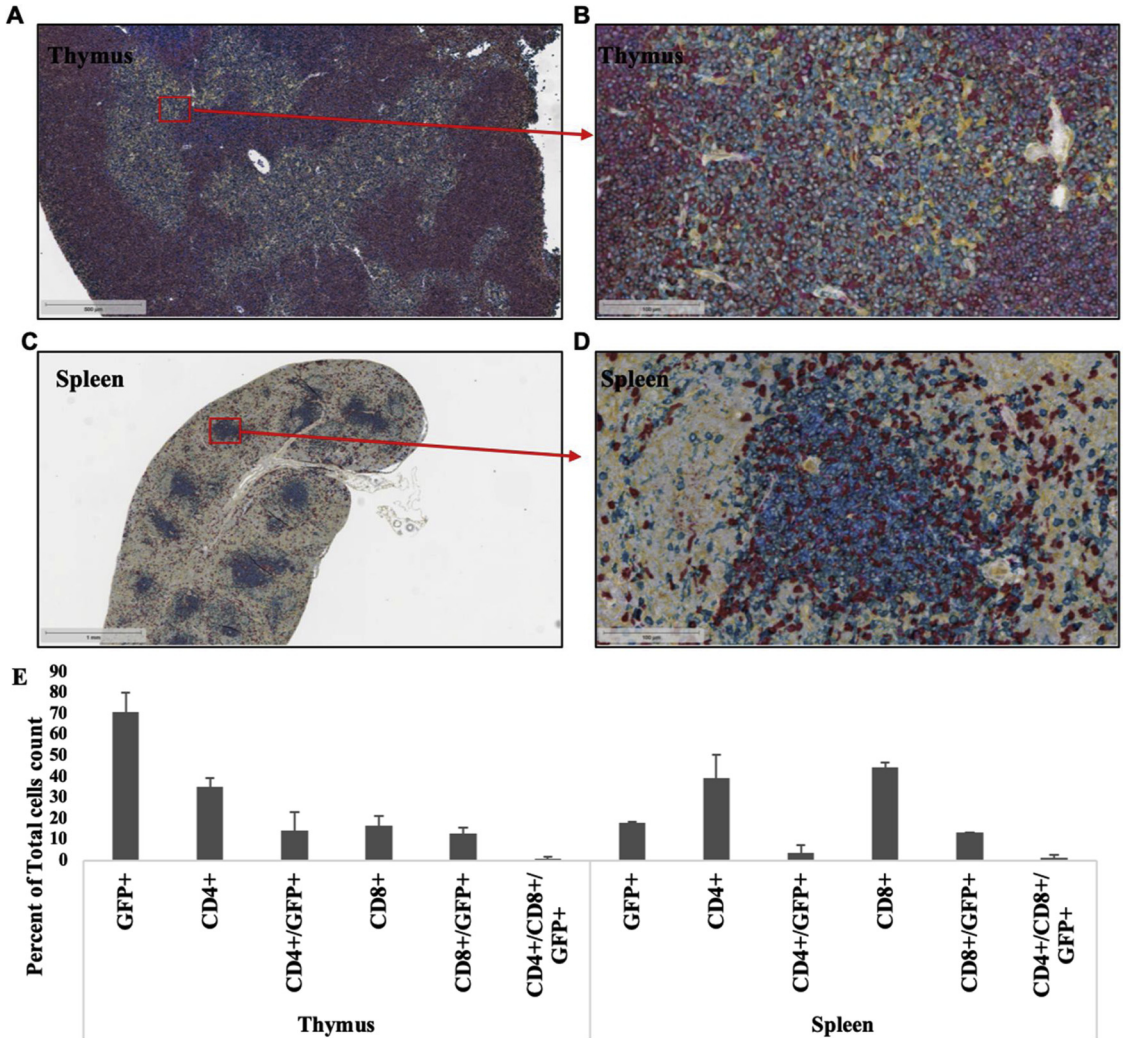

Fig. 5. Immunohistochemistry study of lymphoid tissues sections of (A, B) Spleen and (C, D) Thymus sections, for the detection of CD4 (Teal), CD8 (Purple), GFP (Yellow), Foxp3 (Brown). Colocalization of CD8 + GFP + (Red) is detected in both tissues. CD4 colocalizes with GFP in the Thymus. (E) Percentage of T-cell subpopulations from total cell count in Thymus and Spleen sections. (For interpretation of the references to colour in this figure legend, the reader is referred to the web version of this article).

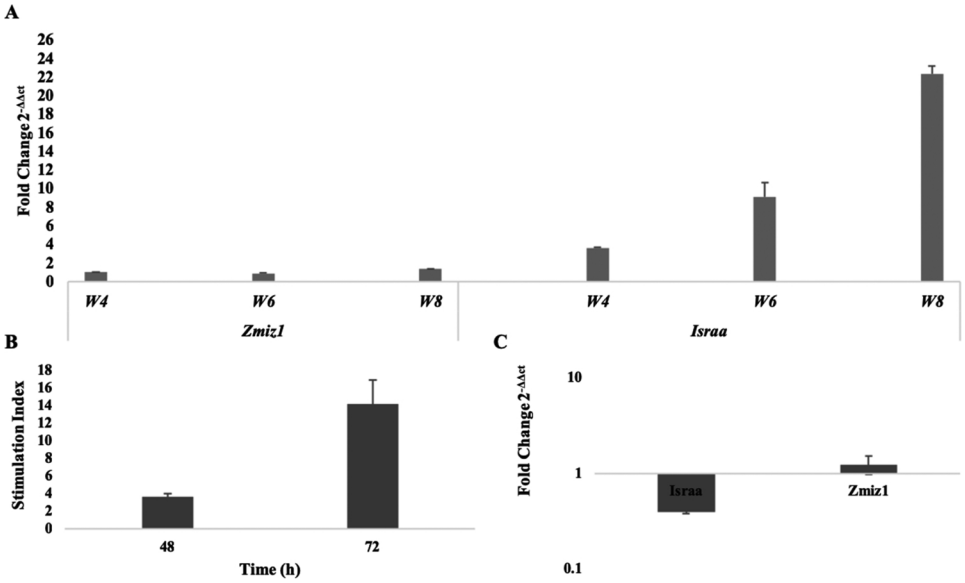

Fig. 6. (A) Real time PCR analysis of *Israa* and *Zmiz1* expression in the Thymus at 4, 6, and 8 weeks aged wild type mice, week4 expression level was used as a reference. (B) Proliferation assay of thymus isolated T-cells after 48 and 72 h of stimulation with anti-CD3/CD28. (C) Real time PCR analysis of *Israa* and *Zmiz1* expression in T-cells stimulated with anti-CD3/CD28 for 48 h. Unstimulated T-cells were used as reference.

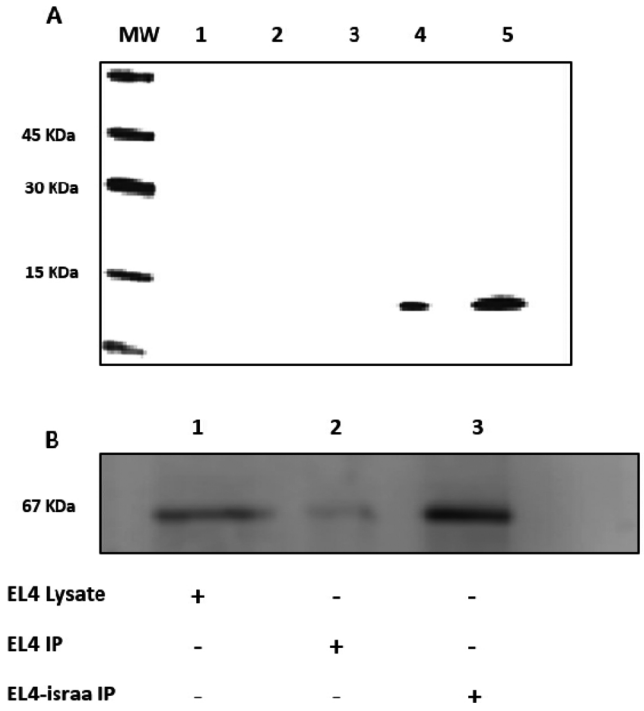

Fig. 7. Analysis of recombinant ISRAA expression and interaction with ELF1. (A) Recombinant ISRAA was expressed in EL4 cells (lanes 2–5). Lane 1: non-electroporated EL4 cells. Cell lysates prepared from 10^4 electroporated EL4 cells (lane 2), 5×10^4 electroporated EL4 cells (lane 3), 10^5 electroporated EL4 cells (lane 4) and 2×10^5 electroporated EL4 cells (lane 5) were subjected to SDS-PAGE and Western blotting with anti-ISRAA antibody. ISRAA is detected as a 15 kDa monomeric protein. (B) Western blot analysis of ELF1 using lysates prepared from non-electroporated EL4 cells (lane 1), non-electroporated EL4 cells were immunoprecipitated with anti-ISRAA antibody (lane 2) and electroporated EL4 cells expressing ISRAA were immunoprecipitated with anti-ISRAA antibody (lane 3). ELF1 was detected at 67 kDa (lanes 1 and 3) and co-immunoprecipitated with ISRAA (lane 3). MW, molecular weight marker, IP, immunoprecipitate.

4. Discussion

We have previously shown that *Israa*, (Ben Khalaf et al., 2016) a novel gene nested within the 50 Kb-long intron 8 of the *Zmiz1* gene, is likely to be involved in T-cell signaling. The host gene, *Zmiz1*, also known as *Zimp10*, encodes for a member of the PIAS (Protein Inhibitor of Activated STAT) family of proteins. PIAS proteins were originally described as repressors of STAT transcription factors and have been shown to function as transcriptional co-regulators that modulate the activity of a diverse set of transcription factors, such as p53, SMADs, and steroid hormone receptors (Sharma et al., 2003). A previous study by Beliakoff and al. showed that *Zmiz1*-deficient embryos die at approximately E10.5 due to severe defects in yolk-sac vessel organization, indicating that *Zmiz1* plays an essential role in the extra-embryonic vascular development process (Beliakoff et al., 2008). It has also been reported that *Zmiz1* is co-expressed with activated *Notch1* across a broad range of T-acute leukaemia oncogenic subgroups (Pinnell et al., 2015). Using a mouse germline in which we have inserted the eGFP coding sequence downstream of the *Israa* gene, we observed that the latter is expressed in lymphoid organs (spleen and thymus) in addition to the brain and testis. Immunohistochemistry and Immunofluorescence confirmed $CD3^+$ cells to express *GFP* in the medulla region of the thymus as well as the spleen white pulp area which demonstrates *Israa*'s expression in both lymphoid tissues T-cells. Stage-specific expression profile was also investigated in the thymus, and interestingly we found *Israa* to be expressed in all stages of T-lymphocyte maturation with different ratios of CD3, CD4 and CD8 markers as indicated in Fig. 5 of the results section. *Israa* expression was associated to $CD3^+$ cells with equal distribution between $CD4^+$ and $CD8^+$ SP cells in the thymus. Only a very small portion of DP ($CD4^+CD8^+$) cells expressed the gene which suggests that *Israa*'s expression occurs mainly in the remaining DN thymocytes. Meanwhile in the spleen, the major subpopulation to express *Israa* are SP CD8+ cells in addition to a small proportion of SP $CD4^+$ cells. These findings suggest that *Israa* regulation displays different profiles depending on the tissues as well as the maturation stage of thymocytes. Indeed, the process of T-cell maturation involves a series of steps that occur independently and sequentially after positive selection. Therefore, the differences observed in the percentages of cells expressing *Israa* within each subpopulation (SP $CD4^+$ and SP $CD8^+$) might be due to fact that cells are not at the same maturation stage. We did not investigate whether B-cells express or not *Israa* gene, but we cannot discard this hypothesis. On another hand, real time PCR experiments confirmed a stage-dependent upregulation of *Israa* expression during developmental stages of the thymus indicating a possible specific role of the gene in this process. Interestingly, no change was observed for the host gene, *Zmiz1*, which suggests an independent expression of the host and the embedded gene. Beside this independent expression regulation, it was also compelling to observe a dissociated regulation between *Israa* and its host gene during T-cell activation following stimulation with anti-CD3/CD28. Indeed, *Israa* was shown to be downregulated in activated T-cells, which suggests negative regulatory role during cell activation. Our findings support the hypothesis that *Israa* is involved in both mechanisms of T-cell development and activation as suggested previously (Ben Khalaf et al., 2016).

Previous analysis (Ben Khalaf et al., 2016) did not reveal any typical regulatory sequences upstream of the *Israa* gene, suggesting that *Israa* may be subject to the same regulatory machinery than *Zmiz1*. Gibson et al. proposed that transcriptional machinery traversing the host gene intron may be subject to steric hindrance from regulatory proteins interacting with the nested gene (Gibson et al., 2005). Although the significance of intronic gene organization in eukaryotic genomes has been investigated in several studies (Gibson et al., 2005; Assis et al., 2008), no correlation in the regulation of intronic and host genes expression was established. Our findings confirm the independent

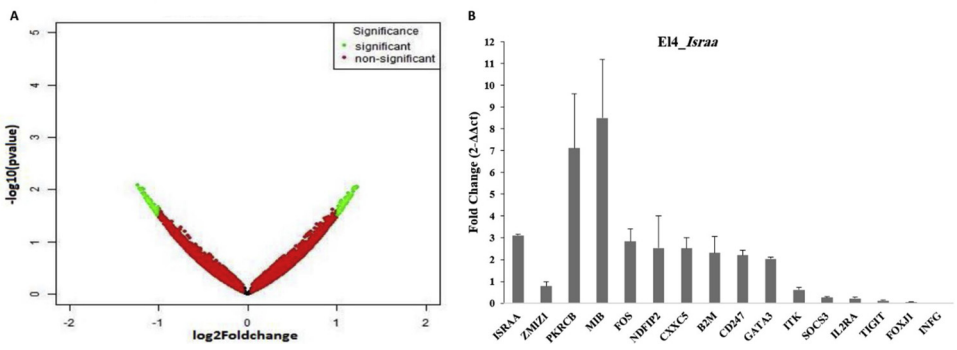

Fig. 8. (A) Volcano Plot of differentially expressed genes in EL4-israa cells compared to mock-transfected EL4 cells. Analysis was performed with Deseq2 software. Significant differentially expressed genes (276) were selected with fold change value between 0.55 and 1.8 and p values ≤ 0.05. (B) Real time PCR validation differential expression of genes involved in T-cell signaling, activation and differentiation. Results are expressed in fold change of gene expression in EL4 cells overexpressing ISRAA compared to mock-transfected cells.

regulation of *Israa* gene from his host gene, but further transcriptomic analysis is needed to investigate the correlation between the two genes.

On the functional level, ISRAA binds to FYN in vivo and the recombinant proteins was shown to regulate anti-CD3-induced T-cell activation as well as the phosphorylation of the Y_{416} residue involved in the activation of Src-family kinases (Ben Khalaf et al., 2016). In this report, we show that ISRAA protein interacts with ELF1, a transcription factor involved in T-cell regulation (Rellahan et al., 1998) and regulates the expression of genes involved in T-cell activation and signaling. T-lymphocytes mainly express two Src-kinase family members, FYN and LCK that play a major role in T-cell signaling. Indeed, knockout mice, deficient in both FYN and LCK were shown to have a profound blockage in T-cell development at the double negative stage (van Oers et al., 1996). Hence, ISRAA might act as a signaling protein following its phosphorylation by FYN. This likeliness is supported by the fact that we validated ELF1 as a binding partner of phosphorylated ISRAA. Indeed, as a member of the *Ets* family of transcription factors, ELF1 plays an important role in T-cell activation and regulation of differentiation (Finco et al., 2006). Interestingly, *Israa*'s host gene, *Zmiz1* was shown also to interact with ETS1, another member of the *Ets* family, and this interaction was shown to be important for regulating Notch1 target genes in T-cell development and leukaemia, such as *Myc* and *Hes1* (Pinnell et al., 2015). This observation suggests that ISRAA could be part of FYN signaling pathway. To our best knowledge, no signaling cascade between FYN and ELF1 has been characterized yet but further functional studies are required to confirm this finding. ELF1 is expressed at high levels in T-cells (Bassuk et al., 1998) and is known to regulate the expression of several T-cell genes including granulocyte-macrophage colony stimulating factor (*GMCSF*) (Wang et al., 1994), interleukin-2 receptor alpha subunit (*Il-2ra*) (Serdobova et al., 1997), *CD4* (Sarafova and Siu, 1999) and the TCR zeta-chain,*CD247* (Rellahan et al., 1998). ELF1 was also shown to positively regulate the expression of the LAT adaptor protein that is central to T-cell receptor signaling (Finco et al., 2006).

With respect to the interaction of ELF1 with ISRAA, the transcriptomic data we generated from the study of the EL4 cell line overexpressing ISRAA, showed that ISRAA overexpression modulates the expression of several genes. Interestingly, among these genes, two were previously reported to be expressed under the regulation of Elf1; *Il2ra* and *CD247*. *Il2ra* known as CD25, which expression is critical for maintaining immune function and homeostasis was shown to be downregulated (Goudy et al., 2013). ELF1 was reported to regulate the expression of the *CD25* gene, which further supports our finding and indicates that ISRAA could play a co-regulation role through ELF1 interaction. Furthermore, *CD25* deficiency is associated with lymphoproliferation and increased T-cell activation markers (Goudy et al., 2013). *CD247*, which plays an important role in coupling antigen recognition by T-cell receptor to several intracellular signal-transduction pathways was also reported to be regulated by Elf1 (Rellahan et al., 1998). Another down-regulated gene is *Itk*, a gene encoding a tyrosine kinase that plays an essential role in regulating the adaptive immune response and the development, function and differentiation of T-cells. *Itk* Knockout mice exhibit defects in the activation, development, and function of $CD4^+$ and $CD8^+$ T-cells and iNKT-cells (Kannan et al., 2015). Interferon-gamma gene, encoding a cytokine associated with anti-proliferative activity (Schroder et al., 2004) was also down-regulated, in addition to the transcription factor *Foxj1*, which has been shown to suppress NFκB signaling (Lin et al., 2004). On the other side, several genes involved in NFκB signaling (*Prkcb*, *Ndfip2*, *Mib2* and *Cxxc5*) were shown to be up- regulated. Other up-regulated genes involved in cell differentiation mainly in the thymus, such as *Gata3* which regulates the development and functions of naive lymphoid cell subsets at multiple stages (Zhu, 2017) and *B2m*, encoding a serum protein found in association with the major histocompatibility complex (MHC) class I heavy chain and involved in the regulation of *CD49f*, an essential factor in thymocyte development (Golbert et al., 2017), might confirm the role of *Israa* in regulating T-cell development and differentiation. Our current data, taken together with the T-cell activation modulation observed previously (Ben Khalaf et al., 2016) points to a potential role for ISRAA in modulating T-cell signaling in activation and differentiation through its phosphorylation by FYN and its interaction with ELF1. Nevertheless, further exploration of cell subsets in lymphoid organs of *Israa* knockout mice and functional studies on NFκB, Notch and Jak-stat signaling and the role of ELF1 in these pathways; should be conducted in mice derived T-cell to further delineate these findings.

This study describes for the first time, an intron-nested gene that is involved in T-cell differentiation and activation. Identification of this gene advances our understanding of the functional importance of intron-nested genes in eukaryotic genomes. Identifying similar genes in human may reveal similar functions that delineate new mechanisms of modulating immune responses. Such findings will enable better understanding of molecular mechanisms regulating immune cell development and activation, and hence set new perspectives for development of immune modulatory approaches.

Acknowledgement

This work was fully funded by a special grant from the Arabian Gulf University, Manama, Kingdom of Bahrain.

References

Assis, R., Kondrashov, A.S., Koonin, E.V., Kondrashov, F.A., 2008. Nested genes and increasing organizational complexity of metazoan genomes. Trends Genet. 24, 475–478.
Baggio, F., Bozzato, A., Benna, C., Leonardi, E., Romoli, O., et al., 2013. 2mit, an intronic gene of Drosophila melanogaster timeless2, is involved in behavioral plasticity. PLoS One 8, e76351.
Bakhiet, M., Taha, S., 2008. A novel nervous system-induced factor inducing immune responses in the spleen. Immunol. Cell Biol. 86, 688–699.
Bartel, P., Chien, C.T., Sternglanz, R., Fields, S., 1993. Elimination of false positives that arise in using the two-hybrid system. Biotechniques 14, 920–924.
Bassuk, A.G., Barton, K.P., Anandappa, R.T., Lu, M.M., Leiden, J.M., 1998. Expression pattern of the Ets-related transcription factor Elf-1. Mol. Med. 4, 392–401.
Beliakoff, J., Lee, J., Ueno, H., Aiyer, A., Weissman, I.L., et al., 2008. The PIAS-like protein Zimp10 is essential for embryonic viability and proper vascular development. Mol. Cell. Biol. 28, 282–292.
Ben Khalaf, N., Taha, S., Bakhiet, M., Fathallah, M.D., 2016. A central nervous system-dependent intron-embedded gene encodes a novel murine Fyn binding protein. PLoS One 11, e0149612.
Benson, D.A., Karsch-Mizrachi, I., Lipman, D.J., Ostell, J., Wheeler, D.L., 2005. GenBank. Nucleic Acids Res. 33, D34–38.
Cawthon, R.M., O'Connell, P., Buchberg, A.M., Viskochil, D., Weiss, R.B., et al., 1990. Identification and characterization of transcripts from the neurofibromatosis 1 region: the sequence and genomic structure of EVI2 and mapping of other transcripts. Genomics 7, 555–565.
Cock, P.J., Fields, C.J., Goto, N., Heuer, M.L., Rice, P.M., 2010. The Sanger FASTQ file format for sequences with quality scores, and the Solexa/Illumina FASTQ variants. Nucleic Acids Res. 38, 1767–1771.
Erlich, Y., Mitra, P.P., delaBastide, M., McCombie, W.R., Hannon, G.J., 2008. Alta-Cyclic: a self-optimizing base caller for next-generation sequencing. Nat. Methods 5, 679–682.
Finco, T.S., Justice-Healy, G.E., Patel, S.J., Hamilton, V.E., 2006. Regulation of the human LAT gene by the Elf-1 transcription factor. BMC Mol. Biol. 7, 4.
Fromont-Racine, M., Rain, J.C., Legrain, P., 1997. Toward a functional analysis of the yeast genome through exhaustive two-hybrid screens. Nat. Genet. 16, 277–282.
Gibson, C.W., Thomson, N.H., Abrams, W.R., Kirkham, J., 2005. Nested genes: biological implications and use of AFM for analysis. Gene 350, 15–23.
Golbert, D.C.F., Santana-Van-Vliet, E., Ribeiro-Alves, M., Fonseca, M., Lepletier, A., et al., 2017. Small interference ITGA6 gene targeting in the human thymic epithelium differentially regulates the expression of immunological synapse-related genes. Cell Adh. Migr. 1–16.
Gotz, S., Garcia-Gomez, J.M., Terol, J., Williams, T.D., Nagaraj, S.H., et al., 2008. High-throughput functional annotation and data mining with the Blast2GO suite. Nucleic Acids Res. 36, 3420–3435.
Goudy, K., Aydin, D., Barzaghi, F., Gambineri, E., Vignoli, M., et al., 2013. Human IL2RA null mutation mediates immunodeficiency with lymphoproliferation and autoimmunity. Clin. Immunol. 146, 248–261.
Hube, F., Francastel, C., 2015. Mammalian introns: when the junk generates molecular diversity. Int. J. Mol. Sci. 16, 4429–4452.
Kannan, A., Lee, Y., Qi, Q., Huang, W., Jeong, A.R., et al., 2015. Allele-sensitive mutant, Itkas, reveals that Itk kinase activity is required for Th1, Th2, Th17, and iNKT-cell cytokine production. Eur. J. Immunol. 45, 2276–2285.
Kumar, A., 2009. An overview of nested genes in eukaryotic genomes. Eukaryot. Cell 8,

1321–1329.
Laird, R.M., Hayes, S.M., 2010. Roles of the Src tyrosine kinases Lck and Fyn in regulating gammadeltaTCR signal strength. PLoS One 5, e8899.
Lee, Y.C., Chang, H.H., 2013. The evolution and functional significance of nested gene structures in Drosophila melanogaster. Genome Biol. Evol. 5, 1978–1985.
Lin, J., Weiss, A., 2001. Identification of the minimal tyrosine residues required for linker for activation of T cell function. J. Biol. Chem. 276, 29588–29595.
Lin, L., Spoor, M.S., Gerth, A.J., Brody, S.L., Peng, S.L., 2004. Modulation of Th1 activation and inflammation by the NF-kappaB repressor Foxj1. Science 303, 1017–1020.
Pinnell, N., Yan, R., Cho, H.J., Keeley, T., Murai, M.J., et al., 2015. The PIAS-like coactivator Zmiz1 is a direct and selective cofactor of Notch1 in t cell development and leukemia. Immunity 43, 870–883.
Rellahan, B.L., Jensen, J.P., Howcroft, T.K., Singer, D.S., Bonvini, E., et al., 1998. Elf-1 regulates basal expression from the T cell antigen receptor zeta-chain gene promoter. J. Immunol. 160, 2794–2801.
Salmeron, J.M., Oldroyd, G.E., Rommens, C.M., Scofield, S.R., Kim, H.S., et al., 1996. Tomato Prf is a member of the leucine-rich repeat class of plant disease resistance genes and lies embedded within the Pto kinase gene cluster. Cell 86, 123–133.
Samelson, L.E., 2002. Signal transduction mediated by the T cell antigen receptor: the role of adapter proteins. Annu. Rev. Immunol. 20, 371–394.
Sarafova, S., Siu, G., 1999. A potential role for Elf-1 in CD4 promoter function. J. Biol. Chem. 274, 16126–16134.
Schroder, K., Hertzog, P.J., Ravasi, T., Hume, D.A., 2004. Interferon-gamma: an overview of signals, mechanisms and functions. J. Leukoc. Biol. 75, 163–189.
Serdobova, I., Pla, M., Reichenbach, P., Sperisen, P., Ghysdael, J., et al., 1997. Elf-1 contributes to the function of the complex interleukin (IL)-2-responsive enhancer in the mouse IL-2 receptor alpha gene. J. Exp. Med. 185, 1211–1221.
Sharma, M., Li, X., Wang, Y., Zarnegar, M., Huang, C.Y., et al., 2003. hZimp10 is an androgen receptor co-activator and forms a complex with SUMO-1 at replication foci. EMBO J. 22, 6101–6114.
Smith-Garvin, J.E., Koretzky, G.A., Jordan, M.S., 2009. T cell activation. Annu. Rev. Immunol. 27, 591–619.
van Oers, N.S., Lowin-Kropf, B., Finlay, D., Connolly, K., Weiss, A., 1996. Alpha beta T cell development is abolished in mice lacking both Lck and Fyn protein tyrosine kinases. Immunity 5, 429–436.
Viskochil, D., Cawthon, R., O'Connell, P., Xu, G.F., Stevens, J., et al., 1991. The gene encoding the oligodendrocyte-myelin glycoprotein is embedded within the neurofibromatosis type 1 gene. Mol. Cell. Biol. 11, 906–912.
Vojtek, A.B., Hollenberg, S.M., 1995. Ras-Raf interaction: two-hybrid analysis. Methods Enzymol. 255, 331–342.
Wang, C.Y., Bassuk, A.G., Boise, L.H., Thompson, C.B., Bravo, R., et al., 1994. Activation of the granulocyte-macrophage colony-stimulating factor promoter in T cells requires cooperative binding of Elf-1 and AP-1 transcription factors. Mol. Cell. Biol. 14, 1153–1159.
Yu, P., Ma, D., Xu, M., 2005. Nested genes in the human genome. Genomics 86, 414–422.
Zhu, J., 2017. GATA3 regulates the development and functions of innate lymphoid cell subsets at multiple stages. Front. Immunol. 8, 1571.